

Article

Assessment of the Influence of Aluminum, Iron, and Manganese Forms on the Phytocenoses of Post-Mining Lands in the Lengerskoye Brown Coal Mine

Akmaral Issayeva ^{1,2}, Waldemar Spychalski ³ , Elżbieta Wilk-Woźniak ² , Dariusz Kayzer ⁴ ,
Radosław Pankiewicz ^{5,*} , Wojciech Antkowiak ⁶ , Bogusława Łeska ⁵ , Akmaral Alikhan ⁷ , Assel Tleukeyeva ⁷
and Zbigniew Rozwadowski ⁸ 

- ¹ Ecology and Biotechnology Institute, Shymkent University, Zhibek Zholy Avenue, 161, Shymkent 160000, Kazakhstan; akmaral.issayeva@bk.ru
 - ² Institute of Nature Conservation, Polish Academy of Science, al. Adam Mickiewicz, 33, 31-120 Krakow, Poland; wilk@iop.krakow.pl
 - ³ Department of Soil Science and Microbiology, Faculty of Agriculture, Horticulture and Biotechnology, Poznan University of Life Sciences, Wojska Polskiego 28 Street, 60-637 Poznan, Poland; waldemar.spychalski@up.poznan.pl
 - ⁴ Department of Mathematical and Statistical Methods, Poznan University of Life Sciences, Wojska Polskiego 28 Street, 60-637 Poznan, Poland; dariusz.kayzer@up.poznan.pl
 - ⁵ Faculty of Chemistry, Adam Mickiewicz University in Poznań, Uniwersytetu Poznańskiego 8, 61-614 Poznan, Poland; bogunial@amu.edu.pl
 - ⁶ Department of Botany, Faculty of Agriculture, Horticulture and Biotechnology, Poznan University of Life Sciences, Wojska Polskiego 28 Street, 60-637 Poznan, Poland; wojciech.antkowiak@up.poznan.pl
 - ⁷ Department of Biotechnology, M. Auezov South Kazakhstan University, Tauke Khan Avenue, 5, Shymkent 160012, Kazakhstan; akmaralka_050393@mail.ru (A.A.); aseltleukeyeva@mail.ru (A.T.)
 - ⁸ Faculty of Chemical Technology and Engineering, West Pomeranian University of Technology in Szczecin, 71-065 Szczecin, Poland; zroz@zut.edu.pl
- * Correspondence: radpan@amu.edu.pl; Tel.: +48-61-829-1798



Academic Editors: Richard

Diaz Alorro, Kazutoshi Haga, Manis Kumar Jha and Md. Mizanur Rahman

Received: 21 October 2024

Revised: 30 January 2025

Accepted: 11 February 2025

Published: 17 February 2025

Citation: Issayeva, A.; Spychalski, W.; Wilk-Woźniak, E.; Kayzer, D.; Pankiewicz, R.; Antkowiak, W.; Łeska, B.; Alikhan, A.; Tleukeyeva, A.; Rozwadowski, Z. Assessment of the Influence of Aluminum, Iron, and Manganese Forms on the Phytocenoses of Post-Mining Lands in the Lengerskoye Brown Coal Mine. *Sustainability* **2025**, *17*, 1642. <https://doi.org/10.3390/su17041642>

Copyright: © 2025 by the authors. Licensee MDPI, Basel, Switzerland. This article is an open access article distributed under the terms and conditions of the Creative Commons Attribution (CC BY) license (<https://creativecommons.org/licenses/by/4.0/>).

Abstract: Post-mining land in areas where mineral extraction has occurred may constitute a significant portion of the land used for various purposes. Such land serves as soil-forming parent material for developing anthropogenic soils, which sometimes exhibit unfavorable physicochemical properties. The toxicity of the waste generated during lignite mining is due to a number of factors, whose determination permits the identification of its origin for the subsequent design of technologies for the waste reclamation. The purpose of the study, in consistence with sustainable development, is to identify the causes of the toxicity of brown coal waste from the Lengerskoye deposit, in southern Kazakhstan. These studies have provided the results essential for planning remedial actions necessary to improve the well-being of the local population, in accordance with the principles of sustainable development. The studies were performed using single extraction; forms of Al, Fe, and Mn; soil texture; elemental analysis; phytocoenosis analysis; and diffractometric, IR spectroscopic, SEM, route reconnaissance, and comparative statistical methods. A decrease in the biodiversity of plant species was noted, with a gradual increase with distance from the waste storage sites. The most resistant plant species in the vicinity of the waste dump were *Cynodon dactylon* (L.) Pers and *Alhagi pseudalhagi* (M. Bieb.) Desv. ex B. Keller & Shap., while *Dodartia orientalis* (L.) was the only plant species found at the edge of the waste dump. The high toxicity of lignite waste is determined by such factors as low pH values, about 3.0; high content of active forms of aluminum, iron, and manganese (344.0, 0.90, and 20 mg/kg); high electrical conductivity—2835 $\mu\text{S}/\text{cm}$; waste composition poor in nutrients; and climate aridity. It has been observed that a content of exchangeable aluminum above 100 mg/kg resulted in an almost complete lack of vegetation.

Keywords: post-mining landscape; physicochemical properties; toxic forms of Al, Fe, and Mn; acidity; phytocenosis; sustainable development of post-mining grounds

1. Introduction

Environmental pollution by various pollutants remains one of the main causes of morbidity and mortality throughout the world [1,2]. The results of numerous studies have revealed a correlative relationship between the ecological state of the environment and quantitative and qualitative indicators of public health, including those at the cytological level [3] and with the reaction of biosphere components [4,5]; however, despite confirmation of the cause-and-effect relationship, further studies are required. The data concerning the causes and nature of toxicity of pollutants contribute to the understanding of the environmental processes, needed for subsequent decision making on the detoxification or neutralization of the effects of toxicants on the environment.

It is known that coal is a product of the microbial bioconversion of plant residues, a process that occurs over millions of years under anaerobic conditions [6,7]. Types of brown coal originating from different deposits and countries are characterized by different toxicities evaluated on the basis of the contents and variety of toxic substances formed upon their combustion. In many countries, coal still remains the main or only source of energy, contributing to the development of the country's economy [8]. On the other hand, the very first step in using this natural resource is an invasion of the equilibrium of the ecological system due to the destruction of soil cover, a decrease in the biodiversity of flora and fauna, changes in water and air conditions, etc. [9,10].

The pollution of the environment with coal waste occurs as a result of erosion processes [11,12]. A multivariate statistical analysis of the data on the impact of mine waters from four open-pit coal mines on the pollution of river sediments revealed a decrease in the concentrations of heavy metals and rare earth elements in areas 100 m downstream from the discharge, which is caused by the washing out of the smallest fractions of bottom sediments by mine waters [13]. In the areas of brown coal mining and waste storage, the physicochemical characteristics of the soil change and its fertility decreases; moreover, damage is caused to surface vegetation with a significant depletion of biodiversity. Due to the processes of water and wind erosion, soil contamination occurs around the areas of brown coal mining and waste storage, where self-healing processes can take a long time [14]. An assessment of the phytotoxicity of soil contaminated with brown coal waste showed that *Lemna minor* L. test plants experienced growth retardation and other phytotoxic effects, which were associated with damage caused by an increase in the production of reactive oxygen species and a decrease in the level of antioxidants [15].

In addition, in the study on the toxicity of coal rocks [16], it was found that black carbon, as a component of particulate matter in the atmosphere, is a product of the incomplete combustion of coal. The organic coating on black carbon particles has been proven to increase their toxicity, manifested by increased genotoxicity and immunosuppression. A seasonal pattern of particulate matter concentrations in the atmosphere has been revealed, with maximum values in winter and increased levels in summer tourist seasons [17]. In addition, a daily dependence was revealed with clear evening and morning peaks due to the heating of residential premises. It has been established that up to 88% of the volume of pollution comes from local sources related to transport, shipping, and agriculture. Further improvement of methods for analyzing the content of coal particles helps to obtain more accurate results and facilitates the interpretation of the data obtained [18]. Similar processes also take place for brown coal particles whose absorption of light initially increased with a

subsequent decreasing trend after the aging of ozone molecules [19]. This observation was explained by changes in organic carbon and oxygen-containing functional groups, and the degradation of polycyclic aromatic hydrocarbons with the subsequent formation of their oxygen-containing forms. According to other studies [20], photochemical aging does not have a serious effect on the absorption of light by coal particles, but depends on the high content of volatile nitrates and organic substances in the environment.

Lignite from Polish deposits contains a large amount of rare and trace elements, which can have a negative impact on the environment and human health [21]. The elements that are toxic at any concentration were identified as lead, mercury, cadmium, beryllium, and arsenic, while those that are toxic at high concentrations included zinc, selenium, copper, and manganese. An increased concentration of manganese, lead, and copper was noted in the ash after coal combustion, which is explained by the low volatility of these elements. The content of cadmium and mercury in the ash was lower, which is due to their high volatility. On the other hand, it was found that the addition of plant waste ash to brown coal ash reduced the content of heavy metals in soil leachates [22].

It has been established that in lignite from one of the Indian deposits, fly ash and ash residue of brown coal belong to class F with the content of $\text{SiO}_2 > \text{Al}_2\text{O}_3 > \text{CaO} > \text{MgO}$ [23]. The content of arsenic, indium, and strontium in the raw materials was higher than in the ash. The content of different elements in the feedstock, fly ash, and bottom ash depended on the degree of volatility of the elements, but their concentrations were within the safe limits of national standards. The mineralogical composition of brown coal from the Indian Barsingar deposit was found to include kaolinite, quartz, and gypsum. The physicochemical characterization of fly ash and brown coal ash permitted the conclusion that the feedstock contained As, In, and Sr [24]. An analysis of a number of lignite samples from the Barmer basin revealed the presence of minerals such as hematite, nepheline, anhydrite, magnesite, andalusite, spinel, and anatase, and a number of minor minerals. The most common compounds were as follows: iron oxide, sulfur oxide, calcium oxide, and quartz, while toxic oxides such as SrO, V_2O_5 , NiO, Cr_2O_3 , Co_2O_3 , and CuO were detected in trace quantities [25].

It is known that brown coal waste stabilizes the state of heavy metals in the soil such as Cr, Pb, and Zn; increases the extractability of metals Cd, Cu, Pb, and Zn; and improves enzyme activity [26]. As a result, humic and fulvic acids acquire a negative charge and, when combined with cations, form organomineral compounds. The presence of toxic elements in brown coal and waste is responsible for different levels of toxicity, which depend on the chemical and mineralogical composition. The direct impact of brown coal waste on soil resources is due to the reduced content of chemical elements, including biogenic ones, which are necessary for plant growth [27]. The indirect impact on the soil is related to its physical properties, i.e., to the fact that brown coal waste has well-developed external and internal surfaces so it shows sorption properties and can act as a natural sorbent [28]. In general, the causes and levels of toxicity of lignite waste are associated with weather-climatic, soil, physicochemical, and biological factors that shape the environment around the waste storage sites of a particular deposit. In this regard, the aim of the study was to determine the content of the active (toxic) forms of aluminum, manganese, and iron in the brown coal waste heaps from the Lengerskoye deposit in southern Kazakhstan.

2. Materials and Methods

The objectives of the study were heaps created of lignite overburden rocks from the Lengerskoye deposit, located in the south of Kazakhstan.

2.1. Weather and Climatic Conditions

The territory of the Turkestan region (TO) is divided into four climatic zones, each of which is characterized by special hydrothermal indicators. In the direction of geographic flow, from the mountains to the lower reaches of the region, several climatic conditions have developed: mountainous, moderately humid, moderately arid, and dry, whose combination is referred to as an arid climate [29]. Precipitation decreases in the same direction from 600 to 150 mm per year. As climate aridity increases, the duration of precipitation decreases. In most of the plain, it is 3–5%; in the foothill zone—9–10%; and in the high mountain zone—17–19%. Annual and monthly precipitation amounts are also variable. According to the South Kazakhstan Center for Hydrometeorology “Kazhydromet”, in the zone of moderately humid climatic conditions, the average annual precipitation can vary from 334.8 to 613.1 mm, and the largest amount occurs in the spring and some autumn and winter months of the year. The months of January and February are characterized by high average monthly amounts of precipitation (121–140 and 33–97 mm, respectively), which are stable over the years. The spring months are inferior in maximum to the winter ones, on average, by 25–35 mm, and their average annual indicators range from 42.3 to 91.1 mm, which is also a pattern across the years; while in November and December, this indicator is variable, in some years there is a complete absence of precipitation in these months. The summer and autumn months—September and October—account for no more than 2.1% of the annual volume of atmospheric moisture. The established distribution of moisture across annual seasons is also typical of the other climatic zones of the region. The south of Kazakhstan is characterized by aridity and the spatiotemporal variability of precipitation. Atmospheric precipitation is strongly seasonal; in most parts of the territory spring and winter peaks predominate, which significantly affects the distribution and dynamics of the migration of pollutants in the environment.

The TO territory has the highest thermal background in Kazakhstan. The summer months are characterized by moisture deficiency and high air temperatures with large daily fluctuations. Temperature differences between the winter minima and summer maxima can range from -30° to $40^{\circ} \pm 4.5^{\circ}\text{C}$. The duration of winter is associated with the instability of the temperature regime when the meridional circulation intensifies and there is an alternation of cold intrusions and the removal of warm air masses from the south; however, the duration of the frost-free period in the region can fluctuate depending on local conditions. Average January temperatures can vary by $13\text{--}14^{\circ}\text{C}$ in the south and $19\text{--}21^{\circ}\text{C}$ in the northwest. In summer, with weakening circulation and an intensely expressed process of heating, the thermal regime is stable. High air temperatures and long summers provide significant thermal resources for the territory. The south of Kazakhstan is characterized by short winters with frequent thaws and precipitation in the form of rain. The change in seasons is associated with the penetration of a cold cyclone from the territory of western Siberia, the Ural-Caspian regions, and a warm anticyclone from the territory of Iran and Afghanistan. The dominant wind roses in the area are in the southwestern and northwestern directions, accounting for 24 and 27%, respectively. In addition, there are stable air currents, called local winds “Altyn Kurek” and “Shakpak”, which regularly repeat in the spring and first summer months of the year, causing spring floods, dry winds, and dust storms.

2.2. Soil Conditions

The soils occurring in the studied area are characterized by significant typological diversity, which is a result of the varied geological and climatic conditions present in the investigated region of southern Kazakhstan [30]. According to the WRB system, the soils in this

area are most commonly classified into the following Reference Soil Groups: Kastanozems, Chernozems, Calcisols, Cambisols, Fluvisols, Solonchaks, Arenosols, and Leptosols.

According to the soil map of Kazakhstan, the soils under the sites where brown coal waste is stored at the Lengerskoye deposit, are classified as Calcisols. Calcisols are characterized by the weak differentiation of the profile into genetic horizons. The upper humus part is divided into two horizons: humus (A) and transitional (AB). Below lies the illuvial carbonate horizon (Bk), which gradually turns into the parent material (C). A common characteristic feature of these soils is a low humus content and a poorly defined macrostructure. Humus, in most cases, is represented by a fulvate composition (the humate–fulvate composition is most clearly expressed only in Czernozems and Haplic Kastanozems. Sufficient porosity (up to 50% of the total volume) is associated with good microaggregation, and the neutral and slightly alkaline reaction of the soils is associated with a well-developed carbonate layer in the lower layers. Under the conditions of a long and dry period, the profile of gray soils is dominated by ascending film-capillary currents, which contribute to the pull-up of carbonates and easily soluble salts to the surface. This process is more pronounced in light gray soils, which is the reason for the increased salinity of the arable layer. The physicochemical properties of gray soils are typical: low absorption capacity (9–10 cmol/kg in light gray soils, 12–15 in typical ones, and up to 18–20 cmol/kg in dark ones), alkaline reaction, and base saturation. The amount of exchangeable K^+ and Na^+ ions is about 2–5% of the capacity. Soil bulk density ranges from 0.5 to 1.7 kg/L. In connection with these properties, medium loamy soils predominate among Calcisols, which are characterized by a high content of silt fraction (0.05–0.005 mm) and which, together with microaggregate particles, form capillary porosity. The provision of gray soils with mobile forms of macroelements, such as phosphorus, nitrogen, and potassium, is average. The content of mobile nitrogen is characterized by a very low indicator—0.2–0.3%. In general, from the agrotechnical point of view, the subtypes of gray soils are characterized as easily compacted, with a sharp decrease in water permeability and the formation of soil crusts after precipitation.

2.3. Description of the Research Object

The subjects of the study were two dumps of post-mining waste localized on the border of the city of Lenger (Figure 1). The waste from the two dumps visually differed in color and structure, so the dumps were referred to as A and B. Dump A was an irregularly shaped hill, up to 15.0 ± 1.2 m high, dark, almost black, sometimes with yellowish-brown color streaks located at 40–50 m from industrial buildings. Waste dump B was a hill of regular, dome-shaped gray color, up to 40.0 ± 2.5 m high, cut from top to bottom by vertical erosion gullies up to 1.0 ± 0.1 m deep and located at 40.0 m from residential buildings.

The samples for analyses were taken from different sites (in four repetitions from each site) with a self-made soil sampler, from the layer of 0–30 cm. The samples from dumps A and B were labeled as follows: A1—initial waste taken from the central part of waste dump A ($42^\circ 11' 22''$ n.l., $69^\circ 52' 05''$ e.l.); A2—waste from the site on the border with dump A ($42^\circ 11' 23''$ n.l., $69^\circ 52' 07''$ e.l.); A3—waste from a small hill 7–8 m from dump A ($42^\circ 11' 24''$ n.l., $69^\circ 52' 04''$ e.l.); B1—initial waste selected from the central part of waste dump B and averaged ($42^\circ 12' 11''$ n.l., $69^\circ 52' 06''$ e.l.); B2—waste from the site located at 3–5 m from the boundaries of dump B ($42^\circ 12' 12''$ n.l., $69^\circ 52' 06''$ e.l.); and B3 waste sample from the site at 30.0 m from the boundaries of dump B ($42^\circ 12' 08''$ n.l., $69^\circ 52' 04''$ e.l.). Prior to the analyses, the samples were dried at room temperature to air-dry condition, shredded, and sieved through 2 mm mesh.



Figure 1. Research object and location of waste sample collection sites (A1, A2, A3, B1, B2, B3) (Google maps): (A)— $42^{\circ}11'23''$ N, $69^{\circ}52'06''$ E; (B)— $42^{\circ}12'11''$ N, $69^{\circ}52'06''$ E.

2.4. Methods of Research

Laboratory studies were carried out on dry material sifted through a sieve with a mesh size of 2 mm. The following analytical methods were used:

- The soil texture was analyzed using the hydrometer method after Casagrande in Prószyński's modification (supplemented with the sieve method to fractionate sand);
- Total CNS was determined by an elementary analyzer Vario Max CNS (Elementar, Langensfeld, Germany);
- Soil pH was measured potentiometrically in 1 mol KCl extract;
- The forms of phosphorus present in the sample were determined in the Olsen extract (0.1 mol/L Na-HCO₃) with the spectroscopic method;

- The present potassium forms were determined in the 1 mol/L $\text{CH}_3\text{COONH}_4$ extract with the ASA method on the Varian Spectra 220FS apparatus.

The extraction of various forms of aluminum, manganese, and iron was carried out according to the procedure shown in Figure 2 [31]. The authors of this reference were concerned with the assessment of potentially active concentrations of aluminum and found out that with both single and sequential extraction, aluminum was released from the interlayer spaces of the studied soils of the Wielkopolska National Park exposed to years of acid rain. Further studies showed that after extraction, together with aluminum, interchangeable active forms Fe_{KCl} , $\text{Fe}_{\text{CuCl}_2}$, Fe_{pyr} , Fe_{oxal} / Mn_{KCl} , $\text{Mn}_{\text{CuCl}_2}$, Mn_{pyr} , and Mn_{oxal} were released.

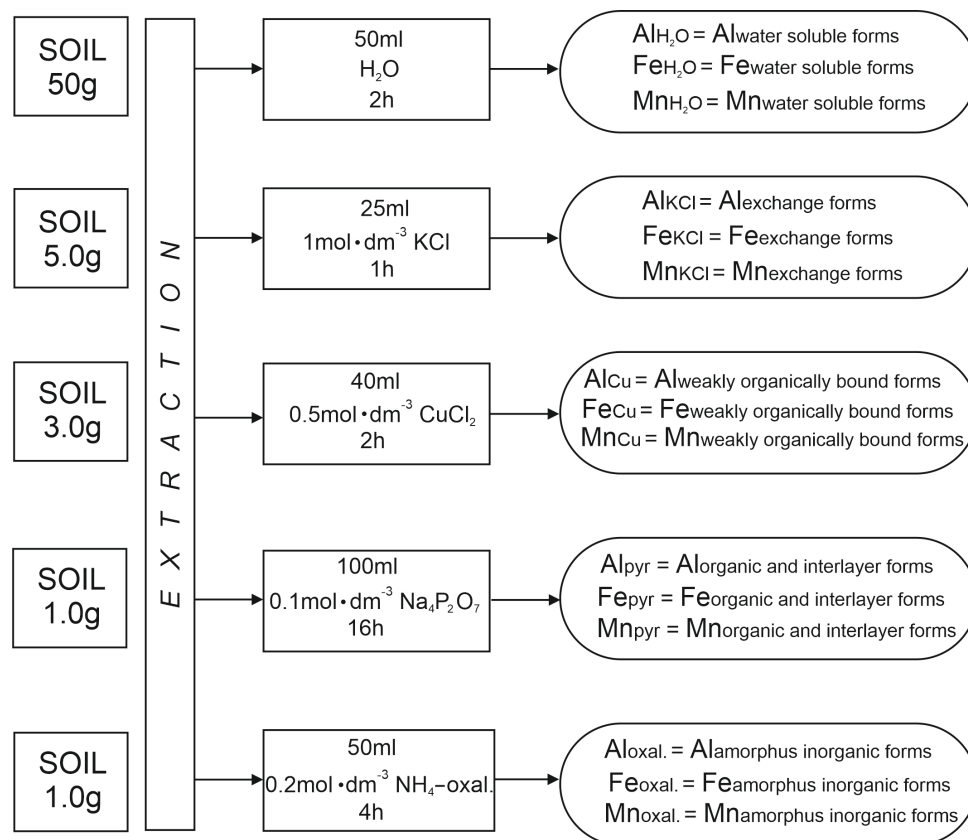


Figure 2. Schematic diagram of the single extraction procedure of different forms of aluminum, iron, and manganese.

The concentrations of Al in the obtained extracts were determined by the atomic absorption spectrometry with atomization in a flame of acetylene/nitrous oxide (iron and manganese in a flame of acetylene/air) using the Varian (Palo Alto, California, U.S.) Spectra 220FS apparatus. The selected soil samples taken from the studied dumps A and B were examined using an S-3700N Hitachi (Tokyo, Japan) scanning electron microscope (SEM) with an EDS Noran SIX system for chemical microanalysis. The samples were operated in low vacuum conditions. Sample A1 was selected for SEM-EDS.

The floristic survey was carried out using the route-reconnaissance method, followed by the desk processing of the collected material. A taxonomic analysis of plants was carried out using the guide “Flora of Kazakhstan” in 9 volumes. The degree of surface coverage with vegetation was determined visually in % ratio: area of vegetation cover/area of the analyzed area. The assessment of the abundance of vegetation in the analyzed areas was carried out on the following scale: 1—single; 2—rare; 3—many; and 4—abundant.

2.5. Statistical Analysis

The differences in the basic chemical properties of the soils and various forms of aluminum, manganese, and iron were determined using a one-way ANOVA. Tukey's method was used for the significance analysis of the differences between the samples of different objects.

For various forms of each element, soil pH, and soil chemical properties, a separate canonical variate analysis (CVA) was conducted, making it possible to visualize the impact of the analyzed metal forms on different groups for each canonical coordinate [32]. These studies were performed because the intergroup and intragroup covariance matrices were analyzed [33]. To study the relationships between the selected objects, the CVA was performed based on transformation by linear combination, and then singular value decomposition was carried out for different forms of elements [34,35]. To compare different objects, the Mahalanobis distances were calculated based on various element forms [36]. In this study, a packages of Excel Microsoft Office, RStudio 2024 and STATISTICA 13 were used for statistical analysis.

3. Results

3.1. Floristic Inspection of Lignite Waste Storage Sites at the Lengerskoye Deposit

An initial inspection of the brown coal waste storage sites showed a difference in the structure of waste in dumps A and B. Waste A from site A1 had a dark, almost black color, anthracite luster, and a dense layered structure, in some places with preserved imprints of leaf veins. Some authors [37] believe that toxicity studies are effective for the preliminary assessment of the safety of coal waste. An initial inspection of the brown coal waste dumps revealed a complete absence of vegetation on the surface of the waste at site A1; however, on the border of the waste area A2, at the base of the dump on the western side, single specimens of *Dodartia orientalis* L. were noted. The area of projective plant coverage of the waste surface ranges from $55.0 \pm 4.5\%$ at site A2 to $80.0 \pm 5.5\%$ at site A3 compared to $90.0 \pm 7.8\%$ of the control area, which was chosen as a site at 500 m from dump A. A decrease in plant species diversity was found from 11 species in the control area to 7 species at site A2, to 4 species at site A3, and, in fact, a complete absence of vegetation at site A1. An analysis of the frequency of occurrence of plants shows that in the control area, *Alhagi pseudalhagi* (Bieb.) Desv. and *Cynodon dactylon* (L.) Pers. were abundantly found, but were eliminated from the phytocenosis at sites A2 and A3 (Figure 3).

These sites were dominated by *Agropyron repens* (L.) P.Beauv., which constitutes the dominant part of the phytocenosis of the areas. At site A2 also the presence of the species *Agropyron cristatum* (L.) Gaertn. was significant, with a frequency of occurrence of three, and *Polygonum aviculare* L. with a frequency of occurrence of two. Waste from dump B is distinguished by its color, varying in shades of gray, and its loose structure with the inclusion of slag-like conglomerates. Around the territory of the city of Lenger, there are more than 10 dumps with a similar shape and slag-like contents. All the dumps of type B have a regular cone-shaped structure, abundantly cut from top to base by vertical erosion gullies, up to 1.0–1.5 m deep. The degree of plant cover in different dumps differs from the complete absence of plants to the partial colonization of plants in the depths of the gullies. In dump B, almost along the entire length of the vertical erosion gullies, *Capparis spinosa* L. was found, which is the only plant species on the highest sections of the gullies (above 15 m). In the sections of the gullies close to the base of the dumps, *Poa bulbosa* L. and *Bromus tectorum* L. appear, which have a depressed appearance and cover small areas under the shoots of *C. spinosa* L. At the sites located 3–5 m from the base of dump B, in addition to *C. spinosa* L. and *Poa bulbosa* L., the species *Achillea millefolium* L., *Agropyron cristatum* L., and *Stipa capillata* L. were noted, which dominate the phytocenosis consisting of the

species of *Centaurea scabiosa* L., *Polygonum aviculare* L., *Capsella bursa-pastoris* (L.) Medik., *Alhagi pseudalhagi* (M.Bieb.) Desv. ex B. Keller & Shap., *Dodartia orientalis* L., *Cousinia* sp., and *Galium album* Mill (Figure 4). In addition, *Peganum harmala* L., *Bromus tectorum* L., and *Althaea officinales* L. were found in single specimens.

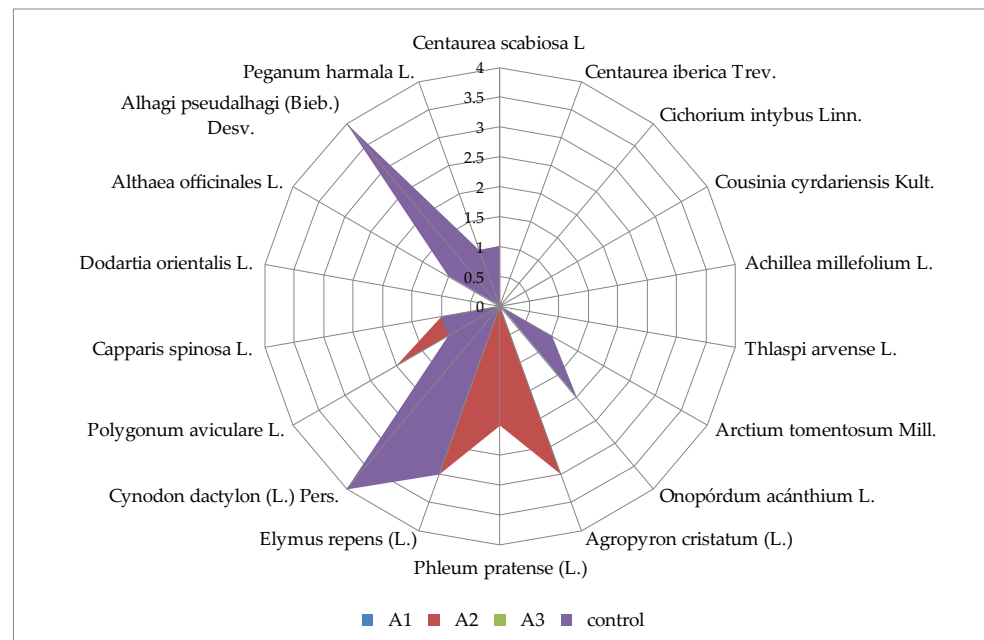


Figure 3. Frequency of occurrence of plants around brown coal waste dump A.

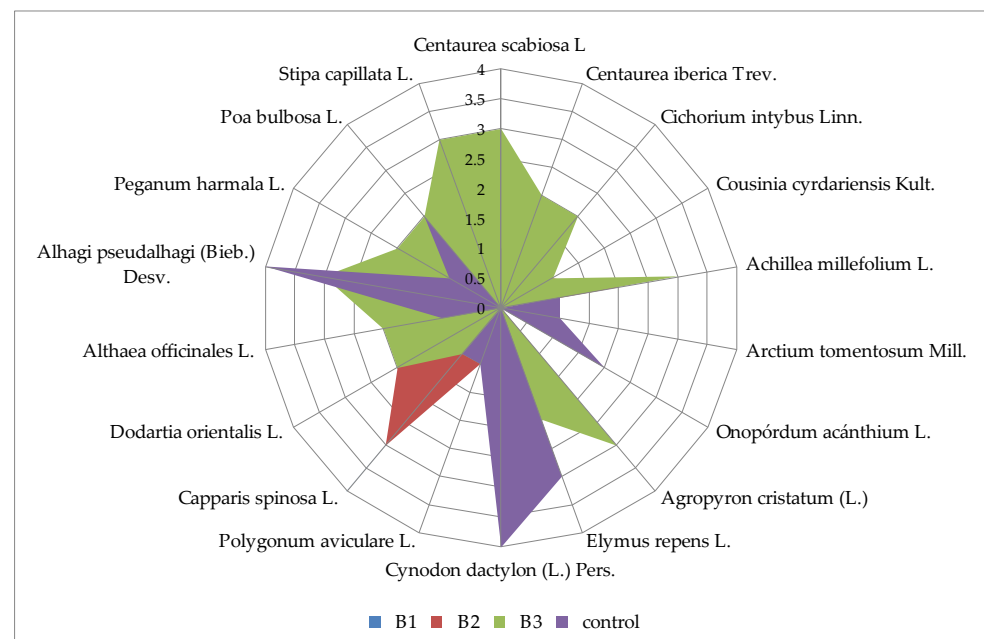


Figure 4. Frequency of occurrence of plants around brown coal waste dump B.

3.2. Physicochemical Characteristics of Brown Coal Waste from the Lengerskoye Deposit

The results of the textural analysis of the studied brown coal waste samples are presented in Figure 5. Their grain size varied and depended on the technological stage of waste formation in the mine. According to the FAO/USDA classification in terms of texture, the waste sample from the A1 site was sandy loam, in which the content of the sand fraction ranged from 63 to 67%, the silt fraction was within 26–32%, and the clay fraction was within 5–7% depending on the size of soil particles. The waste sample from

A2, for the most part, had a sandy loam texture, while its other part was loamy, where the content of the sand fraction dominated and reached 69%, while the content of silt and clay parts ranged from 21 to 37% and 10 to 19%, respectively. The sample from A3 was similar in texture to that from A2 and was classified as sandy and loamy substrates, but differed in the content of the sandy fraction in the range of 36–71%, silty part 19–49%, and clay part 7–15%. The waste samples from dump B, despite the similarity of the textural structure, differed in the composition of soil fractions, so in the sample from B1 of sandy loam and sandy texture, the content of the sand fraction varied in a wide range of 56–88%, that of the silt fraction was within 7–30%, and the clay fraction varied in the range of 5–16%. The sample from B2 revealed a sandy texture with the content of the sand fraction of 89%, while that of the silt and clay parts was up to 10 and 6%, respectively. The sample from B3 had a loamy–sandy and sandy loam texture with a dominance of the sand fraction, occupying up to 82% of the sample volume, the silty part was 13–32%, while the clay part was 5–12%.

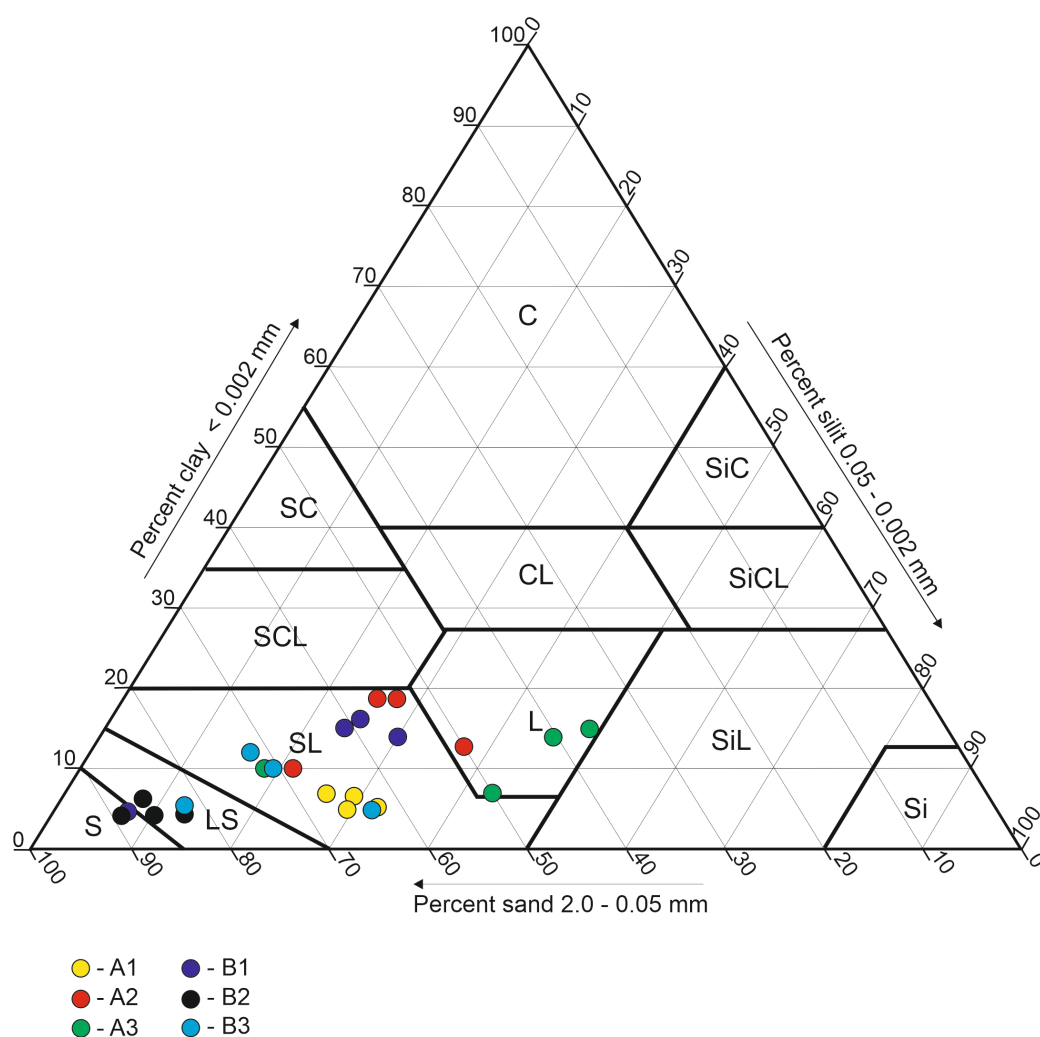


Figure 5. Soil texture of analyzed samples.

An analysis of the percentage content of particular textural fractions revealed a significant differentiation in the contents of all the granulometric fractions and subfractions, which influence all the physical and chemical properties of the formed soils. In the search for the causes of toxicity of brown coal waste from the Lengerskoye deposit, the physicochemical characteristics of the waste: pH values, and nitrogen, carbon, potassium, phosphorus, and sulfur content were determined (Table 1). It was found that the chemical compositions of the analyzed waste samples were also different; however, all the samples were character-

ized by low pH values, which allows these soils to be classified as highly acidic, except for the sample from A3, characterized by neutral or slightly alkaline pH values. This sample also showed the highest nitrogen content, from 0.28 to 0.39%, and a narrower C:N ratio that varied in the range—31–36%.

Table 1. Basic chemical properties (mean \pm standard deviation) in the soil samples taken from the waste brown coals of the Lengerskoje deposit.

Experimental Object	pH	N	C	S	N:S	C:N
		[%]				
A1	2.92 ^a \pm 0.03	0.25 ^b \pm 0.015	13.7 ^b \pm 0.29	0.82 ^b \pm 0.030	0.30 ^b \pm 0.030	56.0 ^b \pm 4.6
A2	4.15 ^b \pm 0.12	0.22 ^b \pm 0.020	13.1 ^b \pm 1.10	0.51 ^a \pm 0.010	0.43 ^{bc} \pm 0.050	60.3 ^b \pm 10.5
A3	7.37 ^d \pm 0.39	0.34 ^c \pm 0.055	11.1 ^b \pm 1.34	0.54 ^a \pm 0.075	0.63 ^c \pm 0.076	33.0 ^a \pm 1.7
B1	3.36 ^a \pm 0.53	0.28 ^{bc} \pm 0.012	12.9 ^b \pm 0.32	0.97 ^b \pm 0.212	0.30 ^b \pm 0.056	45.7 ^{ab} \pm 2.9
B2	3.00 ^a \pm 0.09	0.02 ^a \pm 0.010	1.0 ^a \pm 0.20	0.45 ^a \pm 0.070	0.05 ^a \pm 0.010	44.0 ^{ab} \pm 5.3
B3	5.12 ^e \pm 0.07	0.28 ^{bc} \pm 0.025	12.4 ^b \pm 2.80	0.75 ^{ab} \pm 0.405	0.43 ^{bc} \pm 0.155	44.7 ^{ab} \pm 6.8

Explanation: different lowercase letters denote significant differences in each column ($p < 0.05$).

It was found that the waste samples from different sites differed in both mineralogical and chemical compositions. Microphotographs taken on an X-ray electron microscope showed that the structure of the waste was multifractional with the presence of granules with fuzzy rounded edges (Figure 6). The elemental composition of sample A1 was the closest to that of sample A2. The contents of Al, Fe, K, and Ca in sample A2 differed significantly from those of samples A1 and A3, which allows us to assume a common origin of the latter two.

A thermographic analysis showed that the mineralogical composition of the waste can be described by different ratios of such minerals as gypsum $\text{CaSO}_4 \times 2\text{H}_2\text{O}$, kaolinite $\text{Al}_2\text{Si}_2\text{O}_5(\text{OH})_4$, Margarite $\text{CaAl}_2(\text{Si}_2\text{Al}_2)\text{O}_{10}(\text{OH})_2$, Calcite CaCO_3 , Laumontite $\text{CaAl}_2\text{Si}_4\text{O}_{12}(\text{H}_2\text{O})_2$, silicon oxide SiO_2 , Cronstedtite $\text{Fe}_3((\text{Si}_{0.74}\text{Fe}_{0.26})_2\text{O}_5)(\text{OH})_4$, Muscovite $\text{H}_2\text{KAl}_3(\text{SiO}_4)_3$, and Lead Aluminum Sulfate Hydroxide $\text{Pb}_{0.5}\text{Al}_3(\text{SO}_4)_2(\text{OH})_6$ [33], with a predominance of silicon oxide whose content in the samples ranged from 79.0 to 93.0%.

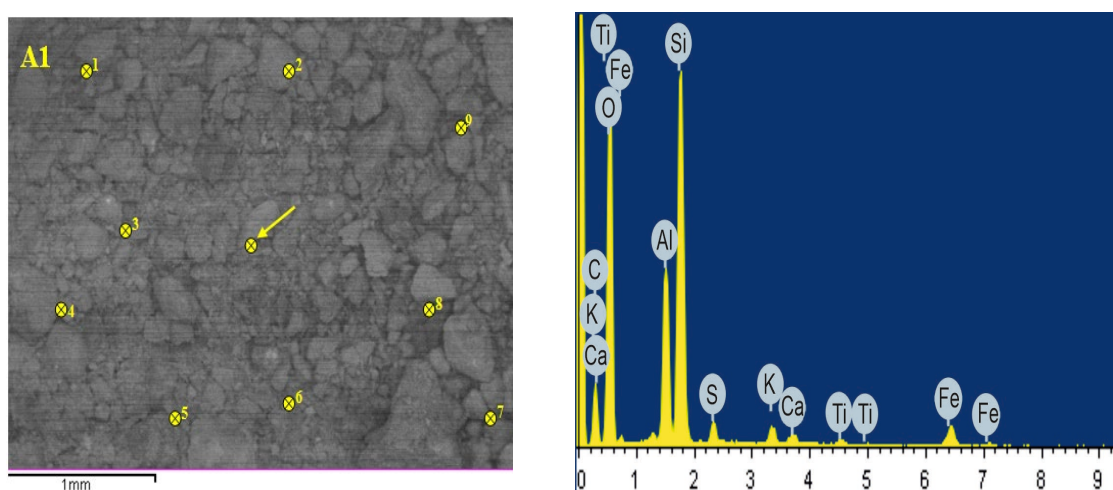


Figure 6. Cont.

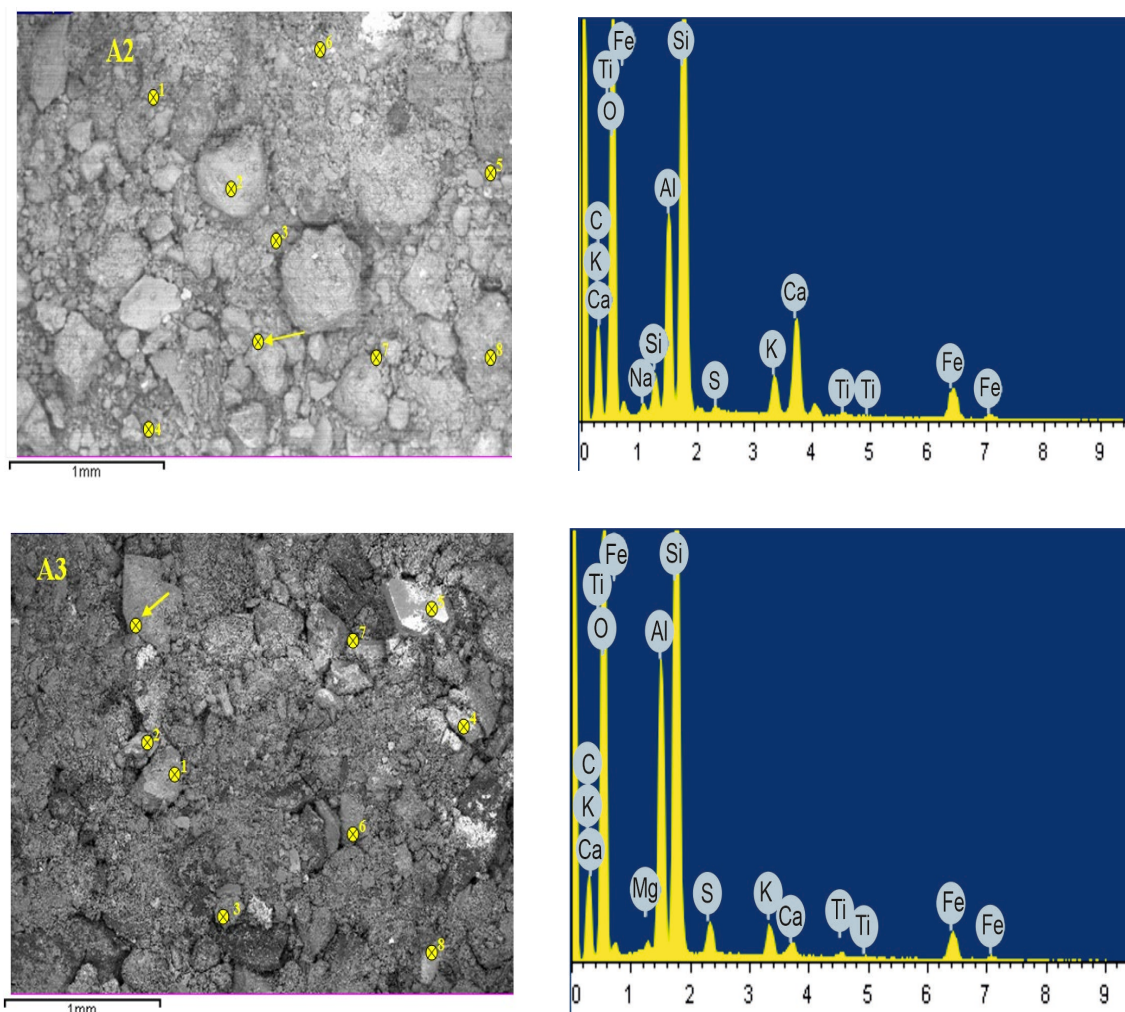


Figure 6. SEM images and EDS spectra of the soil samples analyzed (A1–A3 sample). The yellow points in the microscope photo mark the places where the scans were taken. The arrow marks the point from which the spectrum presented in the image comes from.

3.3. Study of the Causes of Toxicity of Brown Coal Waste from the Lengerskoye Deposit

The contents of the sample components and the sample conductivity varied significantly (Table 2).

Table 2. Electrolytic conductivity (EC) and water-soluble constituents (mean \pm standard deviation) in the soil samples taken from the waste brown coals of the Lengerskoye deposit.

Experimental Object	EC (uS/cm)	Al	Fe	Mn	Mg	Na	K	Ca
		[mg/kg]						
A1	2835.0 ^b \pm 472.6	344.0 ^d \pm 82.7	0.55 ^c \pm 0.03	20.9 ^c \pm 3.2	68.7 ^c \pm 7.3	61.7 ^e \pm 21.2	7.8 ^a \pm 1.2	379.9 ^d \pm 18.9
A2	2348.3 ^b \pm 96.8	70.6 ^c \pm 19.0	0.39 ^{bc} \pm 0.12	16.6 ^{bc} \pm 1.2	26.6 ^b \pm 3.3	20.7 ^d \pm 4.08	10.3 ^{ab} \pm 0.7	238.6 ^a \pm 29.2
A3	491.8 ^a \pm 161.8	1.2 ^a \pm 0.9	0.14 ^a \pm 0.13	0.1 ^a \pm 0.1	14.5 ^a \pm 3.0	3.2 ^b \pm 0.15	12.0 ^b \pm 0.3	56.9 ^b \pm 11.0
B1	2600.0 ^b \pm 113.4	69.8 ^c \pm 3.7	0.90 ^d \pm 0.11	21.5 ^c \pm 4.7	31.5 ^b \pm 4.1	5.6 ^c \pm 1.02	12.5 ^b \pm 1.0	499.7 ^c \pm 68.9
B2	2630.0 ^b \pm 393.2	39.7 ^b \pm 3.1	0.36 ^{bc} \pm 0.04	14.0 ^b \pm 1.7	96.7 ^d \pm 7.8	2.2 ^a \pm 0.09	13.0 ^b \pm 0.5	383.0 ^d \pm 21.1
B3	702.5 ^a \pm 56.7	3.7 ^a \pm 1.0	0.25 ^{ab} \pm 0.03	2.6 ^a \pm 0.6	12.3 ^a \pm 3.0	3.5 ^b \pm 0.44	10.9 ^b \pm 2.6	160.8 ^e \pm 16.4

Explanation: different lowercase letters denote significant differences in each column ($p < 0.05$).

The total manganese content in the lignite waste samples was varied, but a high content of this element was found in combination with organic matter—the Mn_{CuCl_2} fraction in samples A1 and A3, in which the amount of this active form of manganese was several times higher than those in the other samples. The results of our study, presented in Table 2, show that the content of Mn fraction differed statistically significantly depending on the

featured groups. An analysis of the total content of Mn in the tested soil variants revealed that in sample A1, it was higher than in the other ones (Table 3).

Table 3. Manganese fraction content (mean \pm standard deviation) in the soil samples taken from the waste brown coals of the Lengerskoye deposit.

Experimental Object	Mn_{total}	Mn_{H_2O}	Mn_{KCl}	Mn_{CuCl_2}	Mn_{pyr}	Mn_{oxal}
	[mg/kg]					
A1	349.6 ^e \pm 44.2	20.9 ^c \pm 3.2	59.0 ^e \pm 7.6	286.2 ^d \pm 34.8	119.3 ^c \pm 14.5	141.6 ^b \pm 12.3
A2	211.5 ^d \pm 49.4	16.6 ^{bc} \pm 1.2	25.1 ^c \pm 1.7	198.9 ^c \pm 22.9	34.5 ^b \pm 4.0	38.9 ^a \pm 2.3
A3	136.7 ^c \pm 12.9	0.1 ^a \pm 0.1	4.3 ^a \pm 0.7	114.2 ^b \pm 14.2	13.1 ^a \pm 2.1	39.4 ^a \pm 4.8
B1	138.0 ^c \pm 5.9	21.5 ^c \pm 4.7	44.9 ^d \pm 2.6	133.7 ^b \pm 14.7	38.4 ^b \pm 4.7	41.6 ^a \pm 12.1
B2	91.8 ^{ab} \pm 2.7	14.0 ^b \pm 1.7	16.1 ^b \pm 1.7	64.0 ^a \pm 6.0	34.9 ^b \pm 5.8	38.5 ^a \pm 4.5
B3	60.2 ^a \pm 4.4	2.6 ^a \pm 0.6	11.5 ^{ab} \pm 1.9	38.9 ^a \pm 6.8	25.8 ^{ab} \pm 2.4	36.1 ^a \pm 5.6

Explanation: different lowercase letters denote significant differences in each column ($p < 0.05$).

The distributions of discriminant scores across the first and second canonical variables, which together practically account for the variation in the soil samples taken from the brown coal waste dumps of the Lengerskoye deposit, clearly show that the selected samples of various forms of particular elements (Al, Fe, and Mn) are differentiated, suggesting clear boundaries between the areas of certain ground toxicity (Figures 7A, 8A and 9A).

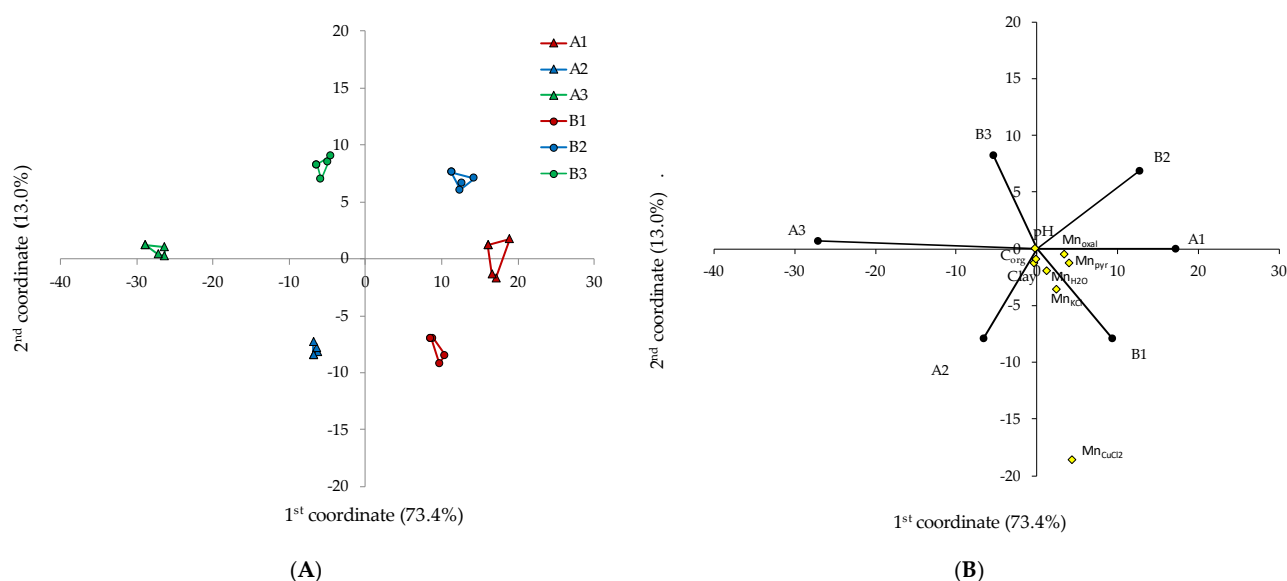


Figure 7. The canonical variate analysis showing the relationship between the selected objects and the content of various species of Mn ((A)—based on transformation by linear combination; (B)—based on singular value decomposition).

The results of the canonical variates analysis based on the comparison of the contents of various forms of Mn, soil pH, and soil chemical properties that describe the selected samples are shown in Figure 7. According to the localization of experimental samples, that is the study area they originated from, the results obtained for samples A1 and B1 were different from those obtained for A3 and B3. The differences were related mostly to the changes in the content of manganese bound to the organic substance (Mn_{CuCl_2} fraction) and manganese bound interchangeably to the soil sorption complex (Mn_{KCl}).

The shortest Mahalanobis distance, calculated on the basis of the contents of various species of Mn, was recorded between samples B2 and B3 (5.68) and then between A3 and B3 (7.49). This means that these groups of samples do not differ significantly in terms of

the contents of different manganese species (Table 4). Additionally, it can be observed that these groups are much less differentiated by pH, Corganic, and clay than by the contents of manganese species. Moreover, the increase in the contents of individual manganese forms was related to the increasing contents of clay and Corganic (Figure 7).

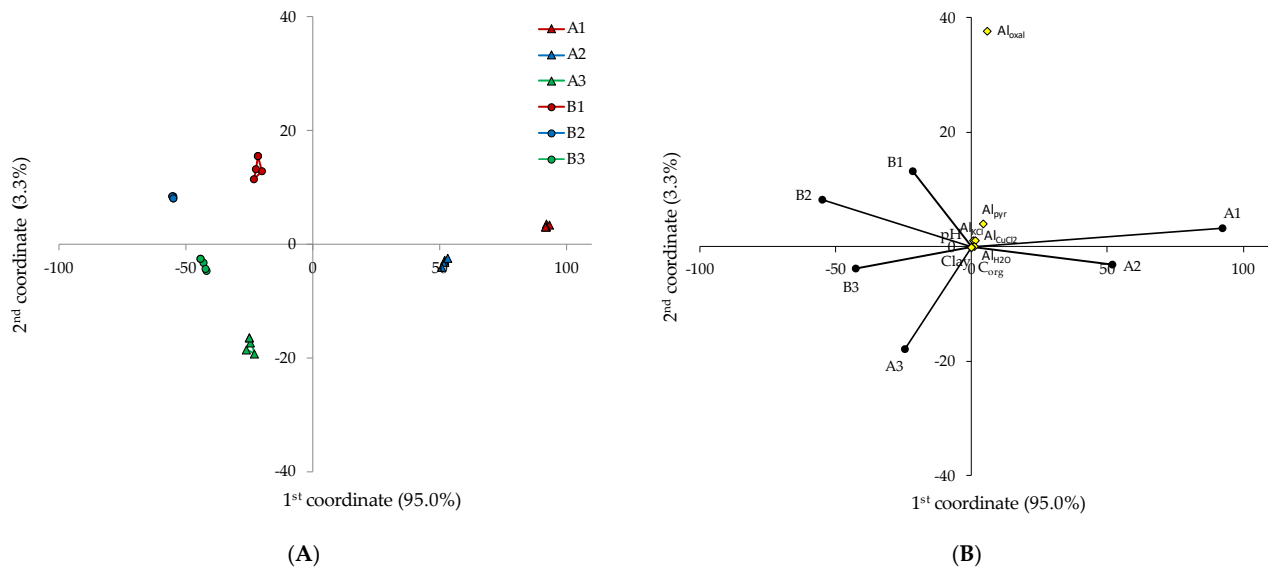


Figure 8. The canonical variate analysis showing the relationship between the selected objects and the content of various species of Al ((A)—based on transformation by linear combination; (B)—based on singular value decomposition).

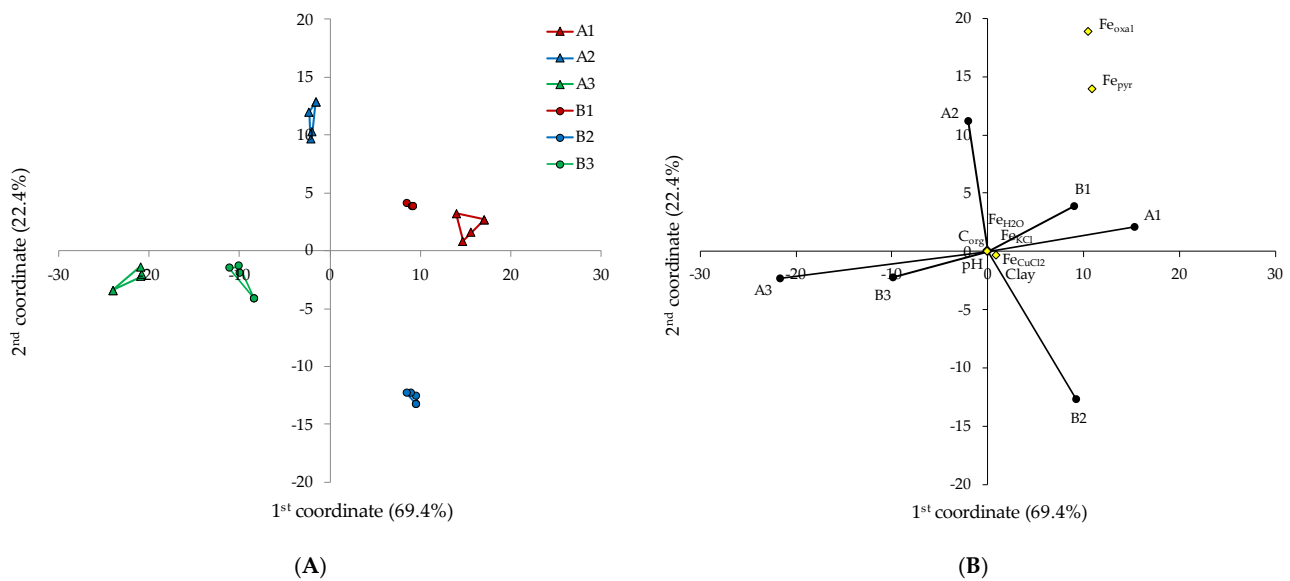


Figure 9. The canonical variate analysis showing the relationship between the selected objects and the content of various species of Fe ((A)—based on transformation by linear combination; (B)—based on singular value decomposition).

A comparative analysis of the contents of different aluminum species showed that in sample A1, the aluminum content significantly exceeds those in the other samples (Table 5). Taking into account the aluminum content in the samples taken from dump A, we can see that the content of exchangeable aluminum—Al_{KCl} fraction in sample A1 exceeded that in sample B1 by 3.7 times, while the aluminum content in the fractions Al_{CuCl2}, Al_{oxal}, and Al_{pyr} exceeded those in sample B1 by 2.2, 3.4, and 1.7 times, respectively. The analysis of the total aluminum content in the tested soil variants showed that in sample A1 it was higher

than in the other samples. Similar total aluminum contents were recorded in samples A2, A3, B2, and B3 (Table 6).

Table 4. Mahalanobis distances between particular objects on the basis of the contents of various species of Mn.

A2	17.69				
A3	20.71	12.68			
B1	17.27	9.85	19.16		
B2	16.16	11.92	9.35	14.65	
B3	18.99	15.56	7.49	18.78	5.68
	A1	A2	A3	B1	B2

Table 5. Mahalanobis distances between particular groups on the basis of active forms of aluminum fraction content.

A2	32.51				
A3	95.56	66.63			
B1	83.74	57.22	28.31		
B2	99.97	71.19	11.72	23.41	
B3	100.68	71.44	10.27	25.59	3.21
	A1	A2	A3	B1	B2

Table 6. Aluminum fraction content (mean \pm standard deviation) in soil samples taken from waste brown coals of the Lengerskoye deposit.

Experimental Object	Al _{total}	Al _{H₂O}	Al _{KCl}	Al _{CuCl₂}	Al _{pyr}	Al _{oxal}
	[mg/kg]					
A1	24,568.4 ^b \pm 4877.4	344.0 ^e \pm 82.7	546.0 ^e \pm 91.1	629.9 ^d \pm 85.7	2040.4 ^e \pm 105.0	4925.3 ^e \pm 298.1
A2	18,518.3 ^a \pm 3618.6	70.6 ^d \pm 19.0	375.8 ^d \pm 39.4	303.2 ^d \pm 8.3	1405.6 ^d \pm 21.4	1476.9 ^c \pm 33.5
A3	16,580.2 ^a \pm 4197.9	1.2 ^a \pm 0.9	1.3 ^a \pm 0.1	177.8 ^c \pm 39.5	131.6 ^b \pm 17.8	158.5 ^a \pm 33.6
B1	21,322.7 ^{ab} \pm 4373.6	69.8 ^d \pm 3.7	107.3 ^c \pm 16.1	140.1 ^c \pm 36.3	587.2 ^c \pm 43.9	4348.2 ^d \pm 398.2
B2	16,051.4 ^a \pm 1012.5	39.7 ^c \pm 2.1	22.3 ^b \pm 3.4	75.1 ^b \pm 6.0	69.6 ^a \pm 5.9	1440.5 ^c \pm 166.1
B3	18,897.7 ^{ab} \pm 872.8	3.7 ^b \pm 1.0	4.5 ^a \pm 0.7	49.8 ^a \pm 9.7	45.8 ^a \pm 6.9	753.5 ^b \pm 67.6

Explanation: different lowercase letters denote significant differences in each column ($p < 0.05$).

An analysis of the CVA results of the content of active forms of aluminum, soil pH, and soil chemical properties presented in Figure 8 shows that the A1 results are significantly different from B2 and B3. This observation was explained by the changes in the content of Al_{oxal} and also those of Al_{pyr} and Al_{KCl}. It can be observed that the increase in Al_{oxal} is related to decreasing pH.

It can be noted that samples B2 and B3 are the closest in terms of the content of aluminum species, as the Mahalanobis distance between them is only 3.21 (Table 5). Further, the Mahalanobis distance increases between the contents of various species of Al, which means that the similarity of its contents in the samples increases, as between samples A3 and B3 it is 10.27, while between samples A3 and B1 it is 28.31. The greatest Mahalanobis difference in the contents of the aluminum species is noted for samples A1 and B3 and it equals 100.68.

The iron contents in the fractions marked as Fe_{oxal} and Fe_{pyr} in sample A1 significantly exceed those in the other samples, but it should be noted that these species are the predominant potentially active forms of iron in all the samples of carbon-containing waste.

The contents of Fe_{KCl} are generally the lowest compared to those of the other iron species and range from 3.0 mg/kg in sample B3 to 15.5 mg/kg in sample A1. The highest Fe_{CuCl_2} content was noted for the samples taken from the sites A1, B1, and B2. Analyzing the total content of iron in the tested soil variants, it was shown that in sample A1, it was higher than in the other ones (Table 7).

Table 7. Iron fraction content (mean \pm standard deviation) in soil samples taken from waste brown coals of the Lengerskoye deposit.

Experimental Object	Fe_{total}	Fe_{H_2O}	Fe_{KCl}	Fe_{CuCl_2}	Fe_{pyr}	Fe_{oxal}
	[mg/kg]					
A1	50,217.4 ^d \pm 1276.9	0.55 ^c \pm 0.03	15.5 ^c \pm 2.2	159.7 ^c \pm 32.3	2477.6 ^d \pm 266.9	2508.6 ^c \pm 274.2
A2	13,265.7 ^b \pm 2400.7	0.39 ^{bc} \pm 0.12	4.5 ^a \pm 0.6	44.5 ^b \pm 1.4	1657.5 ^c \pm 280.7	2167.6 ^b \pm 276.3
A3	17,008.7 ^c \pm 953.7	0.14 ^a \pm 0.13	4.1 ^a \pm 0.6	5.2 ^a \pm 0.7	106.9 ^a \pm 8.2	215.0 ^a \pm 12.5
B1	9573.0 ^a \pm 1458.6	0.90 ^d \pm 0.11	9.3 ^b \pm 2.9	140.1 ^c \pm 11.9	1821.4 ^c \pm 132.6	2021.8 ^b \pm 189.1
B2	9536.0 ^a \pm 704.9	0.36 ^{bc} \pm 0.04	4.5 ^a \pm 0.4	140.7 ^c \pm 10.4	651.0 ^b \pm 61.4	536.1 ^a \pm 90.0
B3	11,825.2 ^{ab} \pm 595.7	0.25 ^{ab} \pm 0.03	3.0 ^a \pm 0.5	12.9 ^a \pm 6.0	169.9 ^a \pm 29.4	151.3 ^a \pm 19.6

Explanation: different lowercase letters denote significant differences in each column ($p < 0.05$).

The results of an analysis of the CVA results concerning the contents of different iron forms, soil pH, and other chemical properties of the soils are presented in Figure 9. The results of the first two canonical coordinates showed that in general, in all the samples, there is a direct correlation between the content of different potentially active forms of iron on the location of the sampling site with an inverse correlation concerning the pH value and percentage of clay content in the samples (Figure 9). This analysis showed that the results obtained for sample A2 were inconsistent with those obtained for sample B2, while the results obtained for sample A3 were inconsistent with those for A1 and B1. The inconsistencies were mainly due to the changes in the iron content in the fractions designated as Fe_{oxal} and Fe_{pyr} . Moreover, similarly to the results for different species of Mn, it can be seen that these samples differed much less in terms of pH, organic carbon, and percentage of clay content. It can be seen that the increase in the content of the Fe_{oxal} and Fe_{pyr} fractions is associated with a decrease in pH. Samples A3 and B3 were characterized by a relatively lower content of organic carbon compared to those in the others.

The greatest similarity in the content of active forms of iron was found for samples A3 and B3, for which the Mahalanobis distance was 1.49. The maximum distance from the readings to the mean values, taking into account the dependence of covariance readings within dump A, was found for sample A1, for which the Mahalanobis distances fluctuated within the range from 17.02 for sample A2 to 18.6 for sample A3. Samples B1, B2, and B3 differed insignificantly in iron content and were within the Mahalanobis distances from 9.98 for samples B2 and B3 to 14.89 for samples B1 and B2, (Table 8).

Table 8. Mahalanobis distances between particular groups on the basis of the contents of various species of Fe.

A2	17.02				
A3	18.16	15.00			
B1	8.41	12.18	15.68		
B2	12.91	18.69	10.48	12.34	
B3	17.83	14.64	1.49	14.89	9.98
	A1	A2	A3	B1	B2

4. Discussion

The results of the floristic study showed that the most stable plant species of phytocenoses around brown coal waste dumps A and B are *Cynodon dactylon* L. and *Alhagi pseudoalhagi* (Bieb.), followed by *Agropyron cristatum* L. and *Erythria repens* L. In general, a comparative analysis of the two dumps shows a decrease in species diversity in all the analyzed sites compared to the control site, with soil uncontaminated by brown coal waste.

The obtained results of the analyses of the physicochemical parameters of the analyzed substrates showed that the soil pH at the analyzed sites was in the range of very acidic, with the exception of sample A3 taken from the site only slightly contaminated with brown coal waste. Extreme pH values, especially for sample A1, may be one of the main causes of the toxicity of these wastes, which is mainly due to the increased concentration of active forms of such elements as aluminum, iron, and manganese.

The organic carbon content in the samples collected from the analyzed research areas reached relatively high values. However, these are not humic compounds but rather the result of admixtures of lignite dust, as evidenced by the wide C:N ratio. The content of phosphorus available for plants in samples A1 and A2 is 4.8 and 8.1 mg/kg P₂O₅, respectively, which is very low. In contrast, in sample A3, the content of available phosphorus was 60.5 mg/kg, so very high.

It is known that one of the metals that form chelate compounds with humic substances is aluminum. When bound to humic acids and fulvic acids, aluminum can no longer bind pentavalent phosphates, which are the phosphorus species available to plants. It was found that in soil containing 1.0% humus, aluminum reduces plant productivity even when present in a content of 1.0 mg/kg of soil. However, when the humus content is increased to 5.0% and above, the aluminum toxicity threshold increases to 15.0 mg/kg of soil. In long-term studies [38] conducted with volcanic soils, it was established that aluminum toxicity is the most important obstacle to plant growth. The toxicity of aluminum in volcanic soils is recognized as an important feature; therefore, it is assigned to a separate subgroup “alic” in the Taxonomy of Soils with a content of KCl-extractable Al >2.0 cmol/kg. It has been established that synthetic aluminum complexes show toxicity and reduce root growth in test plants *Arctium lappa* L. and *Hordium vulgare* L. Moreover, it was found that in the soils in which aluminum–humus complexes or other exchangeable forms of aluminum are formed, this metal becomes highly toxic to root plants. Sample A1 has a very high sulfur content, which is probably converted into sulfuric acid upon oxidation, which consequently causes a decrease in pH (pH 2.67), which further leads to the release of predominantly active aluminum, iron, and manganese which in such an extremely high concentrations are toxic to plants. This is confirmed by the lack of vegetation at this site, and the plant *Dodartia orientalis*, which occurs in single specimens at the border of this site with the base of the dump, is likely to be very resistant to such high concentrations of this form of aluminum.

Many authors have studied the toxicity of various chemical compounds with aluminum such as chloride, hydroxide, nitrate, sulfate, potassium–aluminum alum, aluminum–ammonium alum, silicate, and aluminum phosphate [39,40]. These substances are often used in various processes or products associated with human activities and have been found responsible for a range of dysfunctions of the body, which is a consequence of the high reactivity and availability of aluminum forms [41,42]. Aluminum is known to affect the functions of the reproductive system [43], and cause pathologies in newborns [44] and neurological disorders [45]. It has been established that the toxic effect of aluminum is associated with oxidative stress and impaired lipid peroxidation [46,47], the formation of thrombosis [48], immunosuppressive consequences [49,50], endocrine disorders [51], and the provocation of allergic reactions [52]. The effect of aluminum on plants depends on many factors such as concentration, exposure time, plant type, etc. Despite the fact that

aluminum may be beneficial for plants by mitigating stressful situations, it is not entirely clear what its biological significance is in the cellular systems of plant organisms [53]. Aluminum is considered the main limiting factor that inhibits the development of plants on acidic soils, which is determined by the suppression of root growth, limitation in the consumption of water and nutrients, and changes in the color of individual parts of plants [54]. One way to mitigate the toxic effects of aluminum on plants is to use biochar. According to [55,56], the key properties of biochar that affect the toxicity of aluminum in soil are the process of its production, pyrolysis temperature, pH, electrical conductivity (EC), porosity, ash content, and the presence of various functional groups. The analyzed postmining sediments are characterized by very high electrolytic conductivity, which is a consequence of the high concentration of soluble salts. The results of the study showed that the electrical conductivity of the waste directly correlates with the degree of its toxicity.

Soils containing organic substances with the presence of humic and fulvic acids form low-toxic or non-toxic complex compounds with aluminum, which makes it possible to recommend the use of coal waste containing aluminum in remediation measures [57]. Typically, plants develop the ability to use anions of organic compounds in the form of malates, citrates, and oxalates to detoxify aluminum and replenish phosphorus deficiency. Two pathways for aluminum binding have been described: external, when organic acids outside the cell chelate trivalent aluminum and mobilize phosphorus, and internal, when aluminum is enclosed in a vacuole and phosphorus is released for metabolism [58]. Besides aluminum, iron and manganese are also the most common elements that negatively affect plant growth in acidic soils [59]. Their presence is directly related to soil parameters such as pH, exchangeable acidity, cationic acidity, and the content of organic components. It is known that iron is an element necessary for the growth and development of plants. However, high concentrations of iron in the substrate become toxic as a highly reactive Fenton catalyst [60]. During evolution, plants have developed adaptive strategies aimed at stabilizing the situation with iron deficiency in noncereal plants and the chelation of iron ions in cereal plants [61,62].

Although manganese is needed for plant development as it participates in a number of physiological and metabolic processes, its excess in the soil solution causes the disruption of photosynthesis mechanisms and a decrease in enzyme activity in plants. The protective reaction of plants activates the antioxidant system, regulation of manganese uptake, and sequestration of manganese into intracellular structures [63,64]. For example, a soybean test plant, in response to an excess of manganese, showed a slowdown in growth and an increase in the activity of a number of enzymes, such as superoxide dismutase, catalase, peroxidase, and ascorbate peroxidase, and the content of soluble protein in leaves and roots [65]. In addition, metabolomics analysis based on untargeted liquid chromatography–mass spectrometry identified more than one hundred different metabolites in leaves and roots that responded to manganese toxicity. This suggested that soybean leaves and roots show different types of responses to manganese toxicity, which ultimately leads to the inhibition of plant development. The molecular mechanisms of manganese detoxification in plant organisms have been studied [66].

5. Conclusions

Brown coal waste from the Lengerskoye deposit differs visually and in the origin, which made it possible to divide it into two groups: A-anthracite-like and B-slag-like. The floristic analysis showed a complete absence of plant cover on the surface A1 of dump A. The surface of dump B is covered with vegetation only partially in vertical erosion gullies. For both types of waste, a decrease in the biodiversity of plant species was noted, with its gradual increase with distance from the waste storage sites. The most resistant plant species

around waste dumps A and B are *Cynodon dactylon* L. and *Alhagi pseudoalhagi* (M.Bieb.) Desv. ex B. Keller & Shap., and *Dodartia orientalis* L. was the only plant species found at the border of waste dump A. Based on the results obtained, we can conclude that the causes of phytotoxicity of brown coal waste in the south of Kazakhstan are multifactorial and each factor may enhance the effect of the others. The complex of negative factors that determine the high toxicity of brown coal waste includes the following components: low pH values; high content of active forms of aluminum, iron, and manganese; high electrical conductivity; waste composition poor in nutrients; and climate aridity. High acidification contributed to the release and increased concentration of toxic forms of aluminum. The concentration of exchangeable aluminum above 100 mg/kg resulted in an almost complete lack of vegetation.

Based on the conducted research, it was determined that the primary treatment for the analyzed heaps of post-mining lands should be measures regulating the chemistry of the developing Technosols. These treatments primarily involve neutralizing toxic forms of aluminum, manganese, and iron through liming.

The next stage of land reclamation should involve measures aimed at securing and stabilizing the slopes by planting vegetation that is relatively resistant to the unfavorable chemical conditions of the heaps. Research has shown that the most suitable plants for these plantings are *Dodartia orientalis* L., *Cynodon dactylon*, and *Alhagi pseudoalhagi*.

As a result of these actions, the susceptibility of the developing Technosols to erosion will decrease, significantly improving the well-being of the local community.

Author Contributions: Conceptualization, A.I. and W.S.; methodology, A.I. and W.S.; software, D.K.; validation, W.S., R.P., E.W.-W. and Z.R.; formal analysis, B.L., R.P. and W.A.; investigation, A.I., W.S., A.A. and A.T.; resources, A.A. and A.T.; data curation, A.I. and W.S.; writing—original draft preparation, A.I.; writing—review and editing, W.S., E.W.-W. and R.P.; visualization, W.S., D.K. and R.P.; supervision, A.I., W.S. and R.P.; project administration, E.W.-W. and A.T.; funding acquisition, E.W.-W. All authors have read and agreed to the published version of the manuscript.

Funding: This research was funded by The technology of obtaining organic fertilizers based on the utilization of phosphorus-containing and carbon-containing waste to increase the yield of vegetable crops of the Turkestan region, grant number AP14869410 of Ministry of Science and Higher Education of the Republic of Kazakhstan, and the APC was funded by the Institute of Nature Conservation, Polish Academy of Sciences, within the framework of the grant of the Republic of Kazakhstan “Bolashak-500 scientists”.

Institutional Review Board Statement: Not applicable.

Informed Consent Statement: Not applicable.

Data Availability Statement: Data are contained within the article.

Conflicts of Interest: The authors declare no conflicts of interest.

References

1. Manisalidis, I.; Stavropoulou, E.; Stavropoulos, A.; Bezirtzoglou, E. Environmental and Health Impacts of Air Pollution: A Review. *Front. Public Health* **2020**, *8*, 14. [[CrossRef](#)] [[PubMed](#)]
2. Saurabh, S.; Ankit, Y.; Pallavi, S. Atmospheric Brown Carbon: A Global Emerging Concern for Climate and Environmental Health. In *Management of Contaminants of Emerging Concern (CEC) in Environment*, 1st ed.; Elsevier Science Publishing Co. Inc.: New York, NY, USA, 2021; Volume 8, pp. 225–247. [[CrossRef](#)]
3. Ihtantola, T.; Hirvonen, M.-R.; Ihalainen, M.; Hakkarainen, H.; Sippula, O.; Tissari, J.; Bauer, S.; Di Bucchianico, S.; Rastak, N.; Hartikainen, A.; et al. Genotoxic and inflammatory effects of spruce and brown coal briquettes combustion aerosols on lung cells at the air-liquid interface. *Sci. Total. Environ.* **2021**, *806*, 150489. [[CrossRef](#)] [[PubMed](#)]
4. Yuan, X.; Zhang, X.; Sun, L.; Wei, Y.; Wei, X. Cellular toxicity and immunological effects of carbon-based nanomaterials. *Part. Fibre Toxicol.* **2019**, *16*, 18. [[CrossRef](#)]

5. Gavassi, M.; Alves, F.; Monteiro, C.; Gaion, L.A.; Alves, L.; Prado, R.; Grato, P.; Carvalho, R. Photomorphogenic tomato mutants high-pigment 1 and aurea responses to iron deficiency. *Sci. Hort.* **2023**, *307*, 111502. [CrossRef]
6. Flores, R.M. Coal Composition and Reservoir Characterization. In *Coal and Coalbed Gas Fueling the Future*, 1st ed.; Flores, R.M., Ed.; Elsevier: London, UK, 2014; Volume 3, pp. 235–299. [CrossRef]
7. Wagner, N.J. Geology of Coal. In *Encyclopedia of Geology*, 2nd ed.; Alderton, D., Elias, S.A., Eds.; Academic Press: Oxford, UK, 2021; pp. 745–761. [CrossRef]
8. Szadek, P.; Pająk, M.; Michalec, K.; Wasik, R.; Otremba, K.; Kozłowski, M.; Pietrzykowski, M. The Impact of the Method of Reclamation of the Coal Ash Dump from the “Adamów” Power Plant on the Survival, Viability, and Wood Quality of the Introduced Tree Species. *Forests* **2023**, *14*, 848. [CrossRef]
9. Imran, A.; Maarten, R. Carbonaceous Nanoparticle Air Pollution: Toxicity and Detection in Biological Samples. *Nanomaterials* **2022**, *12*, 3948. [CrossRef]
10. Priyanka, S.; Pallavi, S. Impacts and Responses of Particulate Matter Pollution on Vegetation. In *Airborne Particulate Matter*; Springer: Singapore, 2022; pp. 229–264. [CrossRef]
11. Munawer, M.E. Human health and environmental impacts of coal combustion and post-combustion wastes. *J. Sustain. Min.* **2018**, *17*, 87–96. [CrossRef]
12. Symanowicz, B.; Toczko, R. Brown Coal Waste in Agriculture and Environmental Protection: A Review. *Sustainability* **2023**, *15*, 13371. [CrossRef]
13. Staniszewski, R.; Niedzielski, P.; Sobczyński, T.; Sojka, M. Trace Elements in Sediments of Rivers Affected by Brown Coal Mining: A Potential Environmental Hazard. *Energies* **2022**, *15*, 2828. [CrossRef]
14. Xu, D.; Li, X.; Chen, J.; Li, J. Research Progress of Soil and Vegetation Restoration Technology in Open-Pit Coal Mine: A Review. *Agriculture* **2023**, *13*, 226. [CrossRef]
15. Radić, S.; Medunić, G.; Kuharić, Ž.; Roje, V.; Maldini, K.; Vujčić, V.; Krivohlavak, A. The effect of hazardous pollutants from coal combustion activity: Phytotoxicity assessment of aqueous soil extracts. *Chemosphere* **2018**, *199*, 191–200. [CrossRef] [PubMed]
16. Hakkarainen, H.; Salo, L.; Mikkonen, S.; Saarikoski, S.; Aurela, M.; Teinilä, K.; Ihalainen, M.; Martikainen, S.; Marjanen, P.; Lepistö, T.; et al. Black carbon toxicity dependence on particle coating: Measurements with a novel cell exposure method. *Sci. Total Environ.* **2022**, *838*, 156543. [CrossRef] [PubMed]
17. Milinković, A.; Gregorič, A.; Džaja Grgičin, V.; Vidič, S.; Penezić, A.; Cvitešić Kušan, A.; Alempijević, S.B.; Kasper-Giebl, A.; Frka, S. Variability of black carbon aerosol concentrations and sources at a Mediterranean coastal region. *Atmos. Pollut. Res.* **2021**, *12*, 101221. [CrossRef]
18. Salo, L.; Saarnio, K.; Saarikoski, S.; Teinilä, K.; Barreira, L.M.F.; Marjanen, P.; Martikainen, S.; Keskinen, H.; Mustonen, K.; Lepistö, T.; et al. Black carbon instrument responses to laboratory generated particles. *Atmos. Pollut. Res.* **2024**, *15*, 102088. [CrossRef]
19. Kuang, Y.; Shang, J. Changes in light absorption by brown carbon in soot particles due to heterogeneous ozone aging in a smog chamber. *Environ. Pollut.* **2020**, *266*, 115273. [CrossRef]
20. Cui, F.; Pei, S.; Chen, M.; Ma, Y.; Pan, Q. Absorption enhancement of black carbon and the contribution of brown carbon to light absorption in the summer of Nanjing, China. *Atmos. Pollut. Res.* **2021**, *12*, 480–487. [CrossRef]
21. Bielowicz, B. Selected harmful elements in Polish lignite. *Gospod. Surowcami Miner.—Miner. Resour. Manag.* **2013**, *29*, 47–59. [CrossRef]
22. Vamvuka, D.; Hahladakis, J.; Pentari, D. Leaching of Toxic Elements from Lignite and Agroresidue Ashes in Cultivated Soils of Crete. *Energy Fuels* **2005**, *19*, 807–812. [CrossRef]
23. Lal, R. Soil Conservation and Ecosystem Services. *Int. Soil Water Conserv. Res.* **2014**, *2*, 36–47. [CrossRef]
24. Ram, L.C.; Mastro, R.E.; Srivastava, N.K.; George, J.; Selvi, V.A.; Das, T.B.; Pal, S.K.; Maity, S.; Mohanty, D. Potentially toxic elements in lignite and its combustion residues from a power plant. *Environ. Monit. Assess.* **2015**, *187*, 4148. [CrossRef]
25. Kumar, O.P.; Gopinathan, P.; Naik, A.S.; Subramani, T.; Singh, P.K.; Sharma, A.; Maity, S.; Saha, S. Characterization of lignite deposits of Barmer Basin, Rajasthan: Insights from mineralogical and elemental analysis. *Environ. Geochem. Health.* **2023**, *45*, 6471–6493. [CrossRef] [PubMed]
26. Tsetsegmaa, G.; Akhmadi, K.; Cho, W.; Lee, S.; Chandra, R.; Jeong, C.E.; Wainkwa Chia, R.; Kang, H. Effects of Oxidized Brown Coal Humic Acid Fertilizer on the Relative Height Growth Rate of Three Tree Species. *Forests* **2018**, *9*, 360. [CrossRef]
27. Chen, Y.; Camps-Arbestain, M.; Shen, Q.; Singh, B.; Cayuela, M.L. The long-term role of organic amendments in building soil nutrient fertility: A meta-analysis and review. *Nutr. Cycl. Agroecosyst* **2018**, *111*, 103–125. [CrossRef]
28. Sinitsyna, A.O.; Karnozhitskiy, P.V.; Miroshnichenko, D.V.; Bilets, D.Y. The use of brown coal in Ukraine to obtain water-soluble sorbents. *Sci. Bull. Natl. Min. Univ.* **2022**, *4*, 5–10. [CrossRef]
29. Climate of Kazakhstan. Available online: <https://www.kazhydromet.kz/ru/klimat/klimat-kazahstana-1> (accessed on 29 October 2024).
30. Tarov, A.; Ibraeva, M.A.; Usipbekov, M.; Wilkomirski, B.; Suska-Malawska, M. Brief characteristics of soil cover and analysis of the current state of soil fertility in the South Kazakhstan region. *Soil Sci. Agrochem.* **2008**, *1*, 68–76. (In Russian)

31. Walna, B.; Spychalski, W.; Siepak, J. Assessment of potentially reactive pools of aluminum in poor forest soils using two methods of fractionation analysis. *J. Inorg. Biochem.* **2005**, *99*, 1807–1816. [[CrossRef](#)]
32. Kayzer, D.; Frankowski, P.; Zbierska, J.; Staniszewski, R. Evaluation of trophic parameters in newly built reservoir using canonical variates analysis. In Proceedings of the XLVIII Seminar of Applied Mathematics, Boguszów-Gorce, Poland, 9–11 September 2018; Volume 23, p. 00019. [[CrossRef](#)]
33. Campbell, N.A.; Atchley, W.R. The geometry of canonical variate analysis. *Syst. Biol.* **1981**, *30*, 268–280. [[CrossRef](#)]
34. Czerwińska-Kayzer, D.; Florek, J.; Staniszewski, R.; Kayzer, D. Application of canonical variate analysis to compare different groups of food industry companies in terms of financial liquidity and profitability. *Energies* **2021**, *14*, 4701. [[CrossRef](#)]
35. Kayzer, D.; Czerwińska-Kayzer, D.; Florek, J.; Staniszewski, R. Financial Security as a Basis for the Sustainable Development of Small and Medium-Sized Renewable Energy Companies—A Polish Perspective. *Sustainability* **2024**, *16*, 5926. [[CrossRef](#)]
36. Lejeune, M.; Caliński, T. Canonical Analysis Applied to Multivariate Analysis of Variance. *J. Multivar. Anal.* **2000**, *72*, 100–119. [[CrossRef](#)]
37. Petrović, M.; Fiket, Ž. Environmental damage caused by coal combustion residue disposal: A critical review of risk assessment methodologies. *Chemosphere* **2022**, *299*, 134410. [[CrossRef](#)] [[PubMed](#)]
38. Issayeva, A.U.; Alikhan, A.; Tlegenova, K.; Alpamysova, G.; Issayev, Y.; Tleukeyeva, A. Study of the Possibility of Biorecultivation of Soils Contaminated with Brown Coal Waste. *J. Ecol. Eng.* **2024**, *25*, 314–322. [[CrossRef](#)]
39. Takahashi, T. The diversity of volcanic soils: Focusing on the function of aluminum-humus complexes. *Soil Sci. Plant Nutr.* **2020**, *66*, 666–672. [[CrossRef](#)]
40. Igbokwe, I.O.; Igwenagu, E.; Igbokwe, N.A. Aluminium toxicosis: A review of toxic actions and effects. *Interdiscip. Toxicol.* **2019**, *12*, 45–70. [[CrossRef](#)]
41. Deiab, N.S.; Kodous, A.S.; Mahfouz, M.K.; Said, A.M.; Ghobashy, M.M.; Abozaid, O.A.R. Smart Hesperidin/Chitosan Nanogel Mitigates Apoptosis and Endoplasmic Reticulum Stress in Fluoride and Aluminum-Induced Testicular Injury. *Biol. Trace Elem. Res.* **2023**, *202*, 4106–4124. [[CrossRef](#)]
42. Boran, A.M.; Al-Khatib, A.J.; Alanazi, B.S.; Massadeh, A.M. Investigation of aluminum toxicity among workers in aluminum industry sector. *Eur. Sci. J.* **2013**, *9*, 440–451.
43. Gao, J.; Liu, W.; Pei, J.; Li, J.; Hao, N.; Yang, S.; Yang, X.; Zou, D.; Xu, K.; Zhang, L. The Role of Histone H2B Acetylation Modification in Aluminum-Induced Cognitive Dysfunction. *Biol. Trace Elem. Res.* **2023**, *202*, 3731–3739. [[CrossRef](#)]
44. Mouro, V.G.S.; Menezes, T.P.; Lima, G.D.A.; Domingues, R.R.; Souza, A.C.; Oiveira, J.A.; Matta, S.L.P.; Machado-Neves, M. How bad is aluminum exposure to reproductive parameters? *Biol. Trace Elem. Res.* **2017**, *183*, 314–324. [[CrossRef](#)]
45. Klein, G.L. Aluminum toxicity to bone: A multisystem effect. *Osteoporos. Sarcopenia* **2019**, *5*, 2–5. [[CrossRef](#)]
46. Colomina, M.T.; Peris-Sampedro, F. Aluminum and Alzheimer’s disease. *Adv. Neurobiol.* **2017**, *18*, 183–197.
47. Yang, X.; Yu, K.; Wang, H.; Zhang, H.; Bai, C.; Song, M.; Han, Y.; Shao, B.; Li, Y.; Li, X. Bone impairment caused AlCl₃ is associated with activation of JNK apoptotic pathway mediated by oxidative stress. *Food Chem. Toxicol.* **2018**, *116*, 307–314. [[CrossRef](#)] [[PubMed](#)]
48. Yu, H.; Zhang, J.; Ji, Q.; Wang, P.; Song, M.; Cao, Z.; Zhang, X.; Li, Y. Melatonin alleviates aluminium chloride-induced immunotoxicity by inhibiting oxidative stress and apoptosis associated with the activation of Nrf2 signaling pathway. *Ecotoxicol. Environ. Saf.* **2019**, *173*, 131–141. [[CrossRef](#)] [[PubMed](#)]
49. Hangouche, A.J.E.; Fennich, H.; Alaika, O.; Dakka, T.; Raisouni, Z.; Oukerraj, L.; Doghmi, N.; Cherti, M. Reversible myocardial injury and intraventricular thrombus associated with aluminium phosphide poisoning. *Case Rep. Cardiol.* **2017**, *2017*, 6287015. [[CrossRef](#)]
50. Xu, F.; Ren, L.; Song, M.; Shao, B.; Han, Y.; Cao, Z.; Li, Y. Fas- and mitochondria-mediated signaling pathway involved in osteoblast apoptosis induced by AlCl₃. *Biol. Trace Elem. Res.* **2018**, *184*, 173–185. [[CrossRef](#)] [[PubMed](#)]
51. Gomes, L.S.; Costa, J.R.; Campos, M.S.; Marques, M.R.; Biancardi, M.F.; Taboga, S.R.; Ghedini, P.C.; Santos, F.C.A. Aluminum disrupts the prenatal development of male and female gerbil prostrate (*Meriones unguiculatus*). *Exp. Mol. Pathol.* **2019**, *107*, 32–42. [[CrossRef](#)]
52. Netterlid, E.; Hindsén, M.; Siemund, I.; Björk, J.; Werner, S.; Jacobsson, H.; Güner, N.; Bruze, M. Does allergen-specific immunotherapy induce contact allergy to aluminum? *Acta Derm. Venereol.* **2013**, *93*, 50–56. [[CrossRef](#)]
53. Bojórquez-Quintal, E.; Escalante-Magaña, C.; Echevarría-Machado, I.; Martínez-Estévez, M. Aluminum, a Friend or Foe of Higher Plants in Acid Soils. *Front. Plant Sci.* **2017**, *8*, 1767. [[CrossRef](#)]
54. Ofoe, R.; Thomas, R.H.; Asiedu, S.K.; Wang-Pruski, G.; Fofana, B.; Abbey, L. Aluminum in plant: Benefits, toxicity and tolerance mechanisms. *Front. Plant Sci.* **2023**, *13*, 1085998. [[CrossRef](#)]
55. Sathyaseelan, N.; Karthika, K.S. Aluminium toxicity in soil and plants. *Harit. Dhara* **2019**, *2*, 15–19.
56. Shetty, R.; Vidya, C.S.-N.; Prakash, N.B.; Lux, A.; Vaculík, M. Aluminum toxicity in plants and its possible mitigation in acid soils by biochar: A review. *Sci. Total Environ.* **2021**, *765*, 142744. [[CrossRef](#)]
57. Osman, K.T. *Soils: Principles, Properties and Management*, 1st ed.; Springer: Dordrecht, The Netherlands, 2013. [[CrossRef](#)]

58. Morrissey, J.; Guerinot, M.L. Iron uptake and transport in plants: The good, the bad, and the ionome. *Chem. Rev.* **2009**, *109*, 4553–4567. [[CrossRef](#)] [[PubMed](#)]
59. Nikolic, M.; Pavlovic, J. Chapter 3: Plant responses to iron deficiency and toxicity and iron use efficiency in plants. In *Plant Micronutrient Use Efficiency*; Hossain, M.A., Kamiya, T., Burritt, D.J., Tran, L.P., Fujiwara, T., Eds.; Academic Press: London, UK, 2018; pp. 55–69. [[CrossRef](#)]
60. Zhang, X.; Hui, L.; Shujie, Z.; Juan, W.; Changzhou, W. NH_4^+ -N alleviates iron deficiency in rice seedlings under calcareous conditions. *Sci. Rep.* **2019**, *9*, 12712. [[CrossRef](#)]
61. Aksoy, E. Barley preferentially activates strategy-II iron uptake mechanism under iron deficiency. *Biotech. Stud.* **2024**, *33*, 22–36. [[CrossRef](#)]
62. Noor, I.; Sohail, H.; Zhang, D.; Zhu, K.; Shen, W.; Pan, J.; Hasanuzzaman, M.; Li, G.; Liu, J. Silencing of PpNRAMP5 improves manganese toxicity tolerance in peach (*Prunus persica*) seedlings. *J. Hazard. Mater.* **2023**, *454*, 131442. [[CrossRef](#)]
63. Li, J.; Jia, Y.; Dong, R.; Huang, R.; Liu, P.; Li, X.; Wang, Z.; Liu, G.; Chen, Z. Advances in the Mechanisms of Plant Tolerance to Manganese Toxicity. *Int. J. Mol. Sci.* **2019**, *20*, 5096. [[CrossRef](#)]
64. Wang, Y.; Li, J.; Pan, Y.; Chen, J.; Liu, Y. Metabolic Responses to Manganese Toxicity in Soybean Roots and Leaves. *Plants* **2023**, *12*, 3615. [[CrossRef](#)]
65. Kumar, D.; Kirti, P.B. The genus *Arachis*: An excellent resource for studies on differential gene expression for stress tolerance. *Front. Plant Sci.* **2023**, *14*, 1275854. [[CrossRef](#)]
66. Liu, Y.; Pan, Y.; Li, J.; Chen, J.; Yang, S.; Zhao, M.; Xue, Y. Transcriptome Sequencing Analysis of Root in Soybean Responding to Mn Poisoning. *Int. J. Mol. Sci.* **2023**, *24*, 12727. [[CrossRef](#)]

Disclaimer/Publisher’s Note: The statements, opinions and data contained in all publications are solely those of the individual author(s) and contributor(s) and not of MDPI and/or the editor(s). MDPI and/or the editor(s) disclaim responsibility for any injury to people or property resulting from any ideas, methods, instructions or products referred to in the content.